GeoArabia, v. 15, no. 3, 2010, p. 155-167
Gulf PetroLink, Bahrain

ESSAY

Orbital-forcing glacio-eustasy: A sequence-stratigraphic time scale

Robley K. Matthews and Moujahed I. Al-Husseini

SUMMARY

This essay provides further explanation of the mathematical details of orbital forcing and glacio-eustatic modeling (Parametric Forward Modeling, PFM) aspects and applications. A slight tune-up of the Earth's eccentricity calculations (LA04 of Lasker et al., 2004) produces a near-perfect repeat of 14.58 million-year period and allows PFM to predict the glacio-eustatic component of sea-level fluctuation throughout the Phanerozoic. Generalities of an exploratory grid search of the parameter space of the model are reviewed and repetitive peak sea levels and low sea levels are noted in context of the Arabian Orbital Stratigraphy (AROS) terminology and time scale. Emphasis on the straton (405,000 year "tuning fork" of stratigraphic time) will lead to improvements in sequence-stratigraphic methods and results.

INTRODUCTION

In the course of publishing several papers on the subject of orbital forcing of glacio-eustasy and its relation to sequence stratigraphy (Al-Husseini and Matthews, 2005, 2006, 2008, 2010a, b; Al-Husseini, 2008; Immenhauser and Matthews, 2004), it became apparent that some readers had an interest in technical details beyond the scope of most *GeoArabia* papers. The calculations are indeed unique, and insightful application to Middle East stratigraphy is still evolving rapidly. Technical details are provided here. For snap-shots of an evolving picture yet to be fully unveiled, see Al-Husseini and Matthews (2010a, b).

INSIGHT INTO THE PROBLEM

There is no doubt that the numerical integration of orbital-forcing by Laskar et al. (2004, abbreviated LA04) is an outstanding scientific achievement. However, the astronomer and the stratigrapher have vastly different uses for the orbital-forcing calculations. Basically, the astronomer seeks to understand the precise physics of the Solar System (Sun, planets and their moons), whereas the geoscientist seeks to understand the history of the Earth's ocean-atmosphere-cryosphere system in the context of astronomy and plate tectonics. These differences in purpose between astronomers and stratigraphers become quite clear when it comes to the frequency decomposition of eccentricity.

Math and Physics Approaches

Things begin simple enough. Math is a universal language that describes what we think we see in data or model output. A wiggly curve cannot be described concisely in words. An equation may concisely approximate the wiggly curve, but that does not necessarily imply understanding of *the physics* involved.

Conversely, some *physics* can be said quite well in mere words. For example, in the early 20th Century, Einstein could have said: "If we could convert mass into energy, the energy released would be quite large." Yes! One 100 years ago that was surely an interesting insight that would turn out to be true. But no! Einstein had to write $E = mc^2$ and physicists argued about it for at least 40 years — if not still today! To one outside the field, c^2 (the speed of light, squared) seems virtually unimaginable. Did it ever really get *proved*, or did it just become part of the *common wisdom of physics*?

To the stratigrapher seeking to understand the orbital forcing of the Earth's ocean-atmosphere-cryosphere system, the simple physics can be stated concisely in words: "The gravitational attraction of every planet affects the orbit of every other planet." Indeed, this was the *simple physics* to be tested in the trigonometric expansion of Matthews, Frohlich and Duffy (1997, MFD97). Whereas the representation of eccentricity by Berger and Loutre (1991) involves more than 1,000 terms, MFD97 found 15 simple ($g_{\mathbf{n}}$–$g_{\mathbf{m}}$) terms for all combinations of planets 1 to 6 (Mercury out to Saturn) was sufficient. Interestingly, testing showed four complex Berger and Loutre terms yielded amplitudes comparable to terms 12–15 of MFD97. As a matter of objectivity, and out of deference to Berger and Loutre, these were included in MFD97. For the stratigrapher, the physical meaning of these complex terms almost certainly defies a word-explanation. Such is the slippage from *the physics* into *the math* in problems of interest to the astronomers.

To the astronomer, resonance among the planets is an interesting concept to be worked out in detail (e.g. Laskar et al., 2004, p. 279). The astronomer's first task is to mathematically describe the numerical integration results (e.g. Laskar et al., 2004, their table 4). In table 4 of LA04, the first five terms are readily identifiable as g-values of planets 5, 2, 4, 3 and 1. The physical significance of terms 6, 7, 8 and 11 to 26 is left *yet-to-be-discovered*. The mathematical analysis may even contain fictitious terms resulting from very small errors in the numerical integration or starting conditions. The physics (e.g. resonance, etc.) will come out of careful analysis and/or spectral analysis of overlapping segments of the numerical integration (e.g. 'libration' and 'circulation', Laskar, 1990).

These aspects of orbital forcing are here considered the *math approach*, which is clearly consistent with the astronomer's objectives. It certainly does *explain the data* faster than the MFD97 trigonometric expansion *physics approach*. To a first approximation, *physics* says all planets are interacting with each other. But by the time eleven ($g_{\mathbf{n}}$-$g_{\mathbf{m}}$) terms have been extracted, complex terms of Berger and Loutre (1991) begin to compete, and the amplitude of the eleventh term is still ca. 14% of the first term (e.g. Matthews and Frohlich, 2002, their table 3). In contrast, the eleventh term in Laskar et al. (2004, their table 4) is down to ca. 7% of the first term).

Nevertheless, calculation of orbital-forcing of Earth's eccentricity becomes chaotic after a few tens of millions of years (e.g. Laskar, 1999; Laskar et al., 2004, their figure 23). Small differences in initial conditions produce vastly different estimates of eccentricity on longer time scales. Add in multiple secular resonances among n-planets and their moons and, from an astronomical standpoint alone, this becomes a (nearly?) intractable problem.

To the stratigrapher working on long time scales, the coming, going and/or changing of resonance (libration and circulation) among however many planets can probably be considered noise. As proposed in this essay, a tune-up of LA04 is probably the way to look for long-period repeating patterns that may emerge in the stratigraphic record. In keeping with this philosophy, small differences among simple (g_n-g_m) values and nearly similar μ-values in Laskar et al. (2004, their tables 3, 4 and 6) were not taken under consideration, figuring that the tuning process would probably average out these differences.

Basics of Orbital Forcing

Figures 1 to 3 offer a brief review of the physics of orbital forcing. These figures are reproduced (with slight modification) for the reader's convenience from Matthews and Frohlich (2002). Their paper provides a more thorough introduction to the basics of orbital forcing, especially p. 503–514, and is recommended for interested readers. The numbers are from MFD97 (Matthews, Frohlich and Duffy, 1997) and now slightly changed by LA04. But otherwise, content is still valid and written to be read by stratigraphers.

Based on the rapid Pliocene – Pleistocene glacial advances and retreats in the Northern Hemisphere, some stratigraphers tend to think of the Earth's tilt and precession (periods 18–42 Ky) as governing factors in sequence stratigraphy. Indeed when orbital-forcing data is analyzed with a power-spectrum program, relatively high-frequency tilt and precession show lots of power. This is a *math* result that obscures the *physics* at work. Tilt and precession are high-frequency sampling of *Solstice at Perihelion*

and *Solstice at Aphelion* (Figure 1) of much lower frequency variations in the eccentricity (Figures 2 and 3) of Earth's orbit around the Sun (periods of 95 Ky to 2.4 My to 14.58 My, as explained below).

The *physics* of the ocean-atmosphere-cryosphere system is written in insolation (Watts/m^2) at the Earth's surface. The sea level calculations described below are focused on summer insolation at 70° South and 30° North. At low eccentricity, 70° South summer, insolation is 435 W/m^2 ± 9%; at high eccentricity, 443 W/m^2 ± 22%. Similarly, at low eccentricity, 30° North summer, insolation is 477 W/m^2 ± 5%; at high eccentricity, 483 W/m^2 ± 22%. Indeed, a hint of this is observable in careful power spectrum analysis as *pods* of stronger tilt power (41 Ky) at times of large eccentricity, and less power at times of small eccentricity.

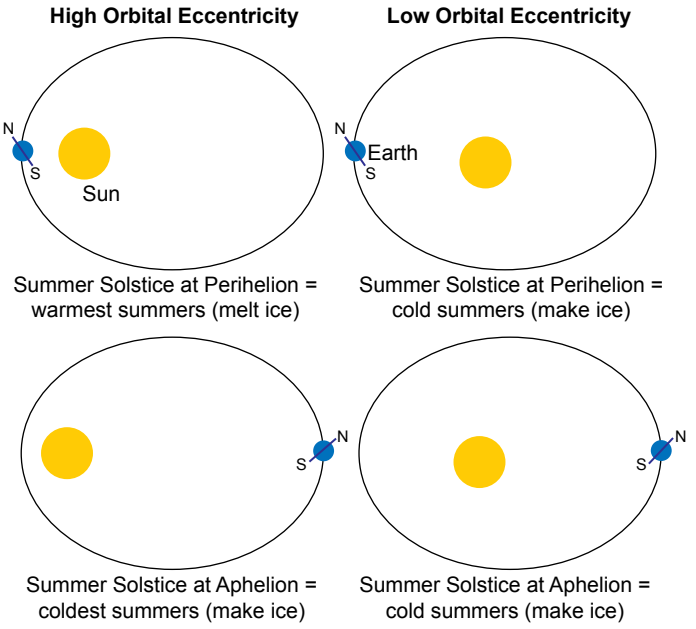

Figure 1: Diagram (not to scale) showing the effect of variations in orbital eccentricity on Antarctic summer insolation. Southern summer solstice at perihelion at a time of high eccentricity is most likely to melt glacial ice. Likewise, given reverse thermohaline circulation, Northern Hemisphere insolation may also affect Antarctic climate by placing warm upwelling water adjacent to a cold continent. See Matthews and Frohlich (2002) for more details.

Figures 2e and 3e plot eccentricity from 2.0–8.0 Ma. Note the relatively smooth, low-amplitude 405 Ky cycles centered at ca. 2.6, 4.6 and 7.4 Ma (green). The 405 Ky cycle is named the "Straton" to distinguish it from empirical sequences that range from 100–500 Ky (Al-Husseini and Matthews, 2010a, b). Stratons can have a complex shape when they modulate the ca. '100 Ky' power as seen in the intervening intervals (Figure 2e and 3e).

TUNING OF LA04 ECCENTRICITY

The eccentricity tune-up concept is based on three observed relationships among the Earth's eccentricity periods (Table 1):

(1) The ca. 2.4 My (g4-g3) Term 6 is very nearly six times the ca. 400 Ky period of the highest amplitude eccentricity Term 1 (g2-g5) (Laskar et al, 2004, their table 6; Matthews and Frohlich, 2002, see Table 1). Likewise, the ca. 2.4 My (g4-g3) modulation of the sum of all ca. '100 Ky' terms (Figure 3d) is very nearly six times Term 1 (405 Ky).

(2) The combination of Planet Mercury terms (Term 7, g1-g5) and (Term 10, g2-g1) produce a complex heterodyne of very nearly 4.8 My repeat interval with an amplitude of nearly 17% of total eccentricity (Figure 4).

(3) When the sum of '100 Ky' terms (e.g. Figure 3d) is run back to 200 Ma, some ca. 2.4 My bundles perfectly retain their '100-Ky' *bundling signature*. This pattern was first noted in calculations comparing changing g-value (e.g. Laskar et al., 1990; cf. Laskar et al., 2004, their figure 9) out-put curves to constant g-value ones. Identical ca. 2.4 My bundling signatures occurred a million or so years apart simply because of differences in age dictated by choice of g-values. This observation implies much of what the astronomer calls *error* can, for the purposes of the stratigrapher, be relegated to cumulative small differences in the time domain. The tune-up of orbital forcing involves making minor modifications to the g-values of LA04 so that these three relationships can be recognized by the stratigrapher throughout the Phanerozoic Era.

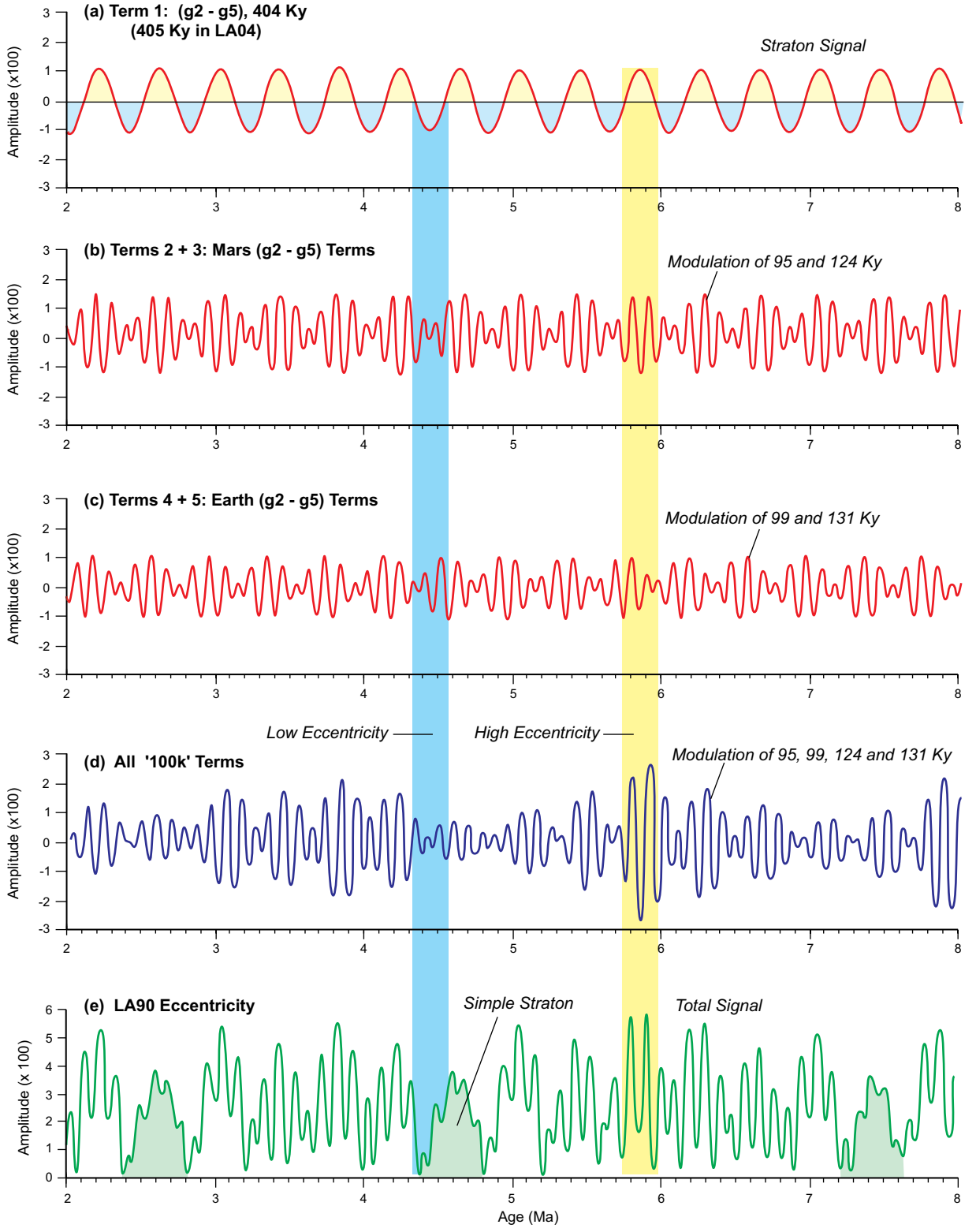

Figure 2: The role of the Straton (405 Ky, g2-g5 in Table 1) in amplitude and amplitude modulation of eccentricity. Panels (a) to (e) are plotted at the same scale for ease of visual comparison. Panel (a) displays the largest single Term 1 in the Fourier calculation of eccentricity (Table 1). Panels (b) and (c) combinations of Mars terms (95 and 125 Ky) and Earth terms (124 and 99 Ky) which modulate with the Straton. Note that low amplitude (blue) in panels (b) and (c) is co-incident with low amplitude in panel (a), and that high amplitude (yellow) in panels (b) and (c) is co-incident with high amplitude in panel (a). The combination of the Straton effect and the Dozon effect (Figure 3) are presented in panel (e). See Table 1 for further clarification of terms 1 through 6. (After Matthews and Frohlich, 2002, with modification).

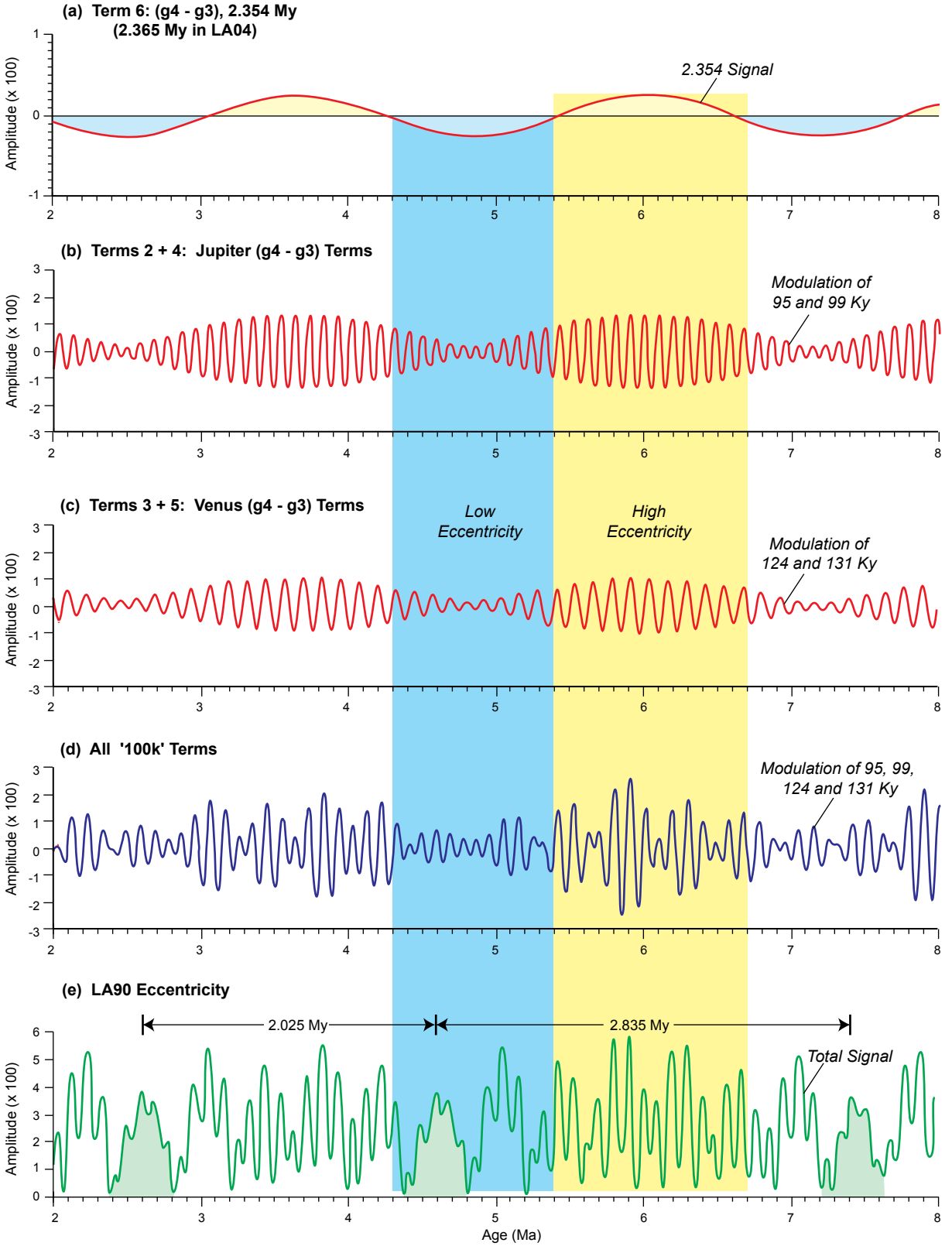

Figure 3: The role of Term 6 (ca. 2.4 My, g4-g3, Table 1) in amplitude and amplitude modulation of eccentricity. Panels (a) to (e) are plotted at the same scale for ease of visual comparison. Panel (a) displays Term 6 in the Fourier calculation of eccentricity (2.365 My in LA04). Panels (b) and (c) combinations of Jupiter terms (95 and 99 Ky) and Venus terms (124 and 131 Ky) which modulates with Term 6. Note that low amplitude (blue) in panels (b), (c) and (d) is co-incident with low amplitude in panel (a), and that high amplitude (yellow) in panels (b), (c) and (d) is co-incident with high amplitude in panel (a). The combination of the Straton effect (Figure 2) and the Dozon effect are presented in panel (e). (After Matthews and Frohlich, 2002, with modification). See Figure 4 and text for further discussion.

Step 1 of Tune-up

To begin, to the reasoning followed here, use of "μ-values" in Laskar et al. (2004), their table 6 is mixing *math* and *physics* approaches. For tuning important to the physics calculation, g3 is substituted for μ6 and g4 for μ7. Fourteen of the 20 terms in Table 1 LA04 column remain as published.

Step 1 is to tune g-values to make these three relationships precise and interlocked. To begin, as suggested by Laskar et al. (2004, p. 261 and 281), Term 1 (g2-g5) is assumed to be precisely 405.000 Ky. The g-values undergoing *tuning* are adjusted plus or minus by an equal amount. Once adjusted, these g-values remain constant through to the end of Step 1.

The sequencing of adjustments to g-values begins with the largest eccentricity Term 1 and makes adjustments at three levels. First, Venus and Jupiter (Term 1, Table 1):

(g2-g5) = 405.000 Ky (1)

Table 1
Results of AROS tune-up of LA04

Term number Laskar et al. (2004). Table 6		LA04 Period (Ky)	Tune-up Period (Ky)	LA04/Tune-up (decimal fraction)
1	g2-g5	405.091	403.611	1.004
2	g4-g5	94.932	94.966	1.000
3	g4-g2	123.945	124.186	0.998
4	g3-g5	98.857	98.842	1.000
5	g3-g2	130.781	130.899	0.999
6	g4-g3	2,364.964	2421.666	0.977
7	g1-g5	977.600	968.667	1.009
8		105.150	105.288	0.999
9		489.694	484.333	1.011
10	g2-g1	688.038	691.905	0.994
11		98.851	98.842	1.000
12		76.909	76.877	1.000
13		130.698	130.899	0.998
14		103.158	103.048	1.001
15		118.077	118.128	1.000
16		109.936	110.074	0.999
17		123.853	124.186	0.997
18		55.002	55.037	0.999
19		94.886	94.966	0.999
20		346.318	345.952	1.001

'g'-values used throughout. See text for discussion.
Average Tune-up >> 0.999
Max longer period, Term 6: +ca. 2.4%
Max shorter period, Term 1: ca - 0.37%

This initial assumption is referred to as Result 1. In subsequent iterations of Steps 1 and 2, this value will be changed. Next, Mars and Earth (Term 6, Table 1):

(g4-g3) = 6 x (405.000) = 2.430 My (2)

Finally, Mercury Term 7 and 10 (Table 1):

(g1-g5) + (g2-g1) = 12 x (405.000) = 4.860 My (3)

Visual inspection of the tuned eccentricity calculation at this initial Step 1 tune-up is both surprising and gratifying. Surprisingly, the *4.8 My near-repeat* is not even close to a repeat regards *405 Ky bundles* of *'100 Ky' peak height signatures*. But gratifying, after (3 x 4.86 = 14.580 My) there is a near-perfect 2.43 My signature repeat; then things drift off again. Thus, 405.000 Ky is not the perfect starting value for this calculation. A second tuning step is required to achieve near-perfect repeat throughout the ca. 14.58 ± x My repeat interval.

Step 2 of Tune-up

Step 2 of the tune-up is to find the precise repeat time interval (ca. 14.58 ± x My) such that all higher-frequency eccentricity terms have precisely a round number of cycles in the repeat interval. Steps 1 and 2 were repeated iteratively to produce a near-perfect repeat, depending on choice of tune-up conceptual model (*math* or *physics*, see below).

At this stage, two tune-ups and related calculated sea-level files were carried forward. First, what is the least change to be done to *LA04-start* (here Laskar et al, 2004, their table 6; Table 1) g-values to achieve a repeat? This is the *math tune-up* question. Iteration of Steps 1 and 2 can indeed produce a near-precise repeat at 70 x (g2-g5) = 12 x (g4-g3) = 28.37046 My. The overall tune-up change in time scale to achieve repeat is ca. + 0.05%. This is referred to as the *math* model because we cannot imagine

physics that would produce a 70 x (ca. 0.405) = ca. 28.37 My repeat. Further, empirically, we also note that long-period stratigraphic sequences tend to be much shorter than ca. 30 My. Nevertheless, when the *math tune-up* of eccentricity is compared to *LA04-start* (correlating maximum and minimum amplitudes of 100 Ky signal), the correlation coefficient is 0.996. The correlation coefficient for MFD97 to LA90 was only 0.95. This improved correlation suggests both Laskar's group and Matthews' group must have been doing some things right in the years 1990 to 2004.

Table 2
Orbiton 1 and AROS Nomenclature

Straton Nominal Age @ base Ma BP	Number from Present	AROS Nomenclature (old)	Predicted Stratigraphic Observations (See grid search text)	AROS 2010 Nomenclature
0.371	1			
0.776	2			
1.181	3			
1.586	**4**	**DS 0.1.1**	**Orbiton sequence boundary**	**DS 0A-1**
1.991	**5**	**DS 1.6.6**	**(Major unconformity)**	**DS 1C-12**
2.396	6	DS 1.6.5		DS 1C-11
2.801	**7**	**DS 1.6.4**	**Lesser MFI**	**DS 1C-10**
3.206	8	DS 1.6.3		DS 1C-9
3.611	**9**	**DS 1.6.2**	**Lesser MFI**	**DS 1C-8**
4.016	10	DS 1.6.1		DS 1C-7
4.421	**11**	**DS 1.5.6**	**Lesser unconformities can occur**	**DS 1C-6**
4.826	**12**	**DS 1.5.5**		**DS 1C-5**
5.231	13	DS 1.5.4		DS 1C-4
5.636	14	DS 1.5.3		DS 1C-3
6.041	**15**	**DS 1.5.2**	**Major MFI**	**DS 1C-2**
6.446	**16**	**DS 1.5.1**	**Dozon unconformities**	**DS 1C-1**
6.851	**17**	**DS 1.4.6**	**can be Orbiton-scale SBs**	**DS 1B-12**
7.256	18	DS 1.4.5		DS 1B-11
7.661	**19**	**DS 1.4.4**	**Lesser MFI**	**DS 1B-10**
8.066	20	DS 1.4.3		DS 1B-9
8.471	**21**	**DS 1.4.2**	**Lesser MFI**	**DS 1B-8**
8.876	22	DS 1.4.1		DS 1B-7
9.281	**23**	**DS 1.3.6**	**Lesser unconformities can occur**	**DS 1B-6**
9.686	**24**	**DS 1.3.5**		**DS 1B-5**
10.091	25	DS 1.3.4		DS 1B-4
10.496	26	DS 1.3.3		DS 1B-3
10.901	**27**	**DS 1.3.2**	**Major MFI**	**DS 1B-2**
11.306	**28**	**DS 1.3.1**	**Dozon unconformities**	**DS 1B-1**
11.711	**29**	**DS 1.2.6**	**can be Orbiton-scale SBs**	**DS 1A-12**
12.116	30	DS 1.2.5		DS 1A-11
12.521	**31**	**DS 1.2.4**	**Lesser MFI**	**DS 1A-10**
12.926	32	DS 1.2.3		DS 1A-9
13.331	**33**	**DS 1.2.2**	**Lesser MFI**	**DS 1A-8**
13.736	34	DS 1.2.1		DS 1A-7
14.141	**35**	**DS 1.1.6**	**Lesser unconformities can occur**	**DS 1A-6**
14.546	**36**	**DS 1.1.5**		**DS 1A-5**
14.951	37	DS 1.1.4		DS 1A-4
15.356	38	DS 1.1.3		DS 1A-3
15.761	**39**	**DS 1.1.2**	**Major MFI**	**DS 1A-2**
16.166	**40**	**DS 1.1.1**	**Orbiton sequence boundary**	**DS 1A-1**
16.571	**41**	**DS 2.6.6**	**(Major unconformity)**	**DS 2C-12**
16.976	42	DS 2.6.5		DS 2C-11

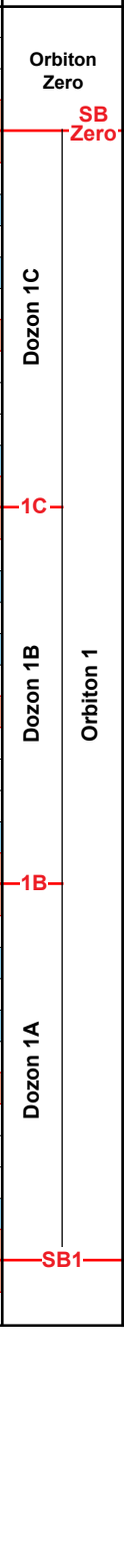

We can imagine (but cannot prove) *physics* that would produce a near-perfect repeat at 36 x (g2-g5) = 6 x (g4-g3) = 14.580 My, assuming (g2-g5) = 405.000 Ky. The actual *physics tune-up* iteration result is (g2-g5) = 403.6 Ky and a 14.530 My repeat interval. The overall tune-up change in time scale to achieve repeat is thus ca. - 0.37% (ca. 50 Ky per 14.5 My years). The *physics tune-up* results are provided in Table 1. Regards precision, the Step 1, Step 2 iteration ultimately alters Laskar et al. (2004) Table 6 terms 1 through 20 such that each term fits a whole number of cycles into a 14.530 My repeat interval to ± 2 in the fourth decimal place (as in 14.5298 ≈ 14.530 My). Likewise, all 20 estimates of Term 1 (g2-g5) (i.e. (14.53 nm/36)) converge on 0.4036 My with a zero or a one in the fifth decimal place.

Regards a *time-scale standard*, we defer to the suggestion of Laskar et al. (2004, p. 261 and 281) so that the *physics* time scale is converted to an AROS standard *tuning fork* time scale of 405.000 Ky equals one Straton, 12 stratons equal one 4.86 My "Dozon" and 36 stratons equal one 14.58 My "Orbiton" (Al-Husseini and Matthews, 2010a; Table 2).

The reason for the discrepancy between Laskar et al. (2004) proposed generality (g2-g5) = 405.000 Ky and the tuned (g2-g5) = 403.611 Ky may lie in *libration and circulation* (Laskar, 1990) among *n* planets; *n* being greater than one, but less than six. This might be a discrepancy of interest to astronomers; but with

$$405.0000/403.611 = 1.00344 \qquad (4)$$

the difference is inconsequential to the present state of biostratigraphy and stratigraphic geochronology.

As an interesting aside, note that the *physics model* concept of 6 x (g2-g5) = (g4-g3) = 2.43 My does not appear in Figures 2e or 3e. Rather, as shown in Figure 3e, to the left of 4.6 Ma, there is a simple, low-amplitude Straton repeated at ca. 2.6 Ma (being: 5 x g2-g5) = 2.025 My) and to the right of 4.6 Ma, a simple, low-amplitude Straton repeated at ca. 7.4 Ma (being: 7 x (g2-g5)= 2.835 My). The Mercury terms are likely responsible for this alternating pattern of 2.0 My third-order cycle followed by one 2.8 My third-order cycle.

As illustrated in Figure 4, the Mercury terms peak structure at ca. 3.0 ± 1.5 Ma is perfectly repeated at ca. 7.9 ± 1.5 Ma (yellow), whereas the structure at valleys in the Mercury terms similar to the one at ca. 5.5 ± 1.5 Ma are upside-down, reverse images of the adjacent peaks structures (blue). Note also that phasing with Term 1 (g2-g5) is reinforcing at ca. 3.0 and 7.8 Ma, but of opposite sign at ca. 5.5 Ma. At around ca. 5.5 Ma, reinforcement by other terms produces alternating third-order terms consisting of 5 x 405 Ky and 7 x 405 Ky. Resultant 405 Ky nodes of reduced '100 Ky' power are noted in both LA04 and the tune-up at ca. 2.6 Ma, 4.6 Ma, 7.4 Ma and so alternating (5 x 405 Ky), (7 x 405 Ky) back in time in the tune-up model. This is the likely origin of the observed Dozon (12 x 405 Ky = 4.86 My) in Al-Husseini and Matthews (2010a).

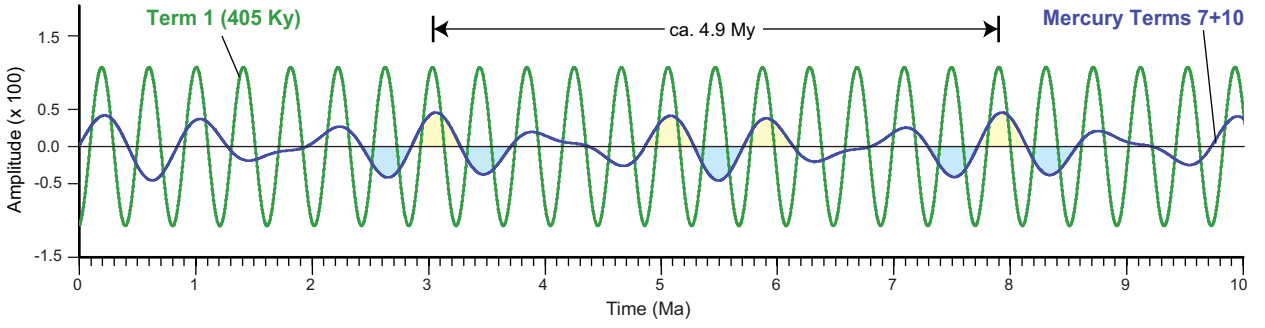

Figure 4: Graph depicting the relation between LA04 Fourier Term 1 and the sum of Mercury terms 7 and 10. Note that the sum of these Mercury terms, [(g1-g5) + (g2-g1)] has a repeat interval of ca. 4.9 My (most easily seen as peak and coincidence with Term 1 peaks at ca. 3.0 and 7.9 Ma). Note also that Mercury curve lows at 2.6 and 7.4 Ma coincide with low-amplitude stratons depicted in panel (e) of Figures 2 and 3. See text for discussion.

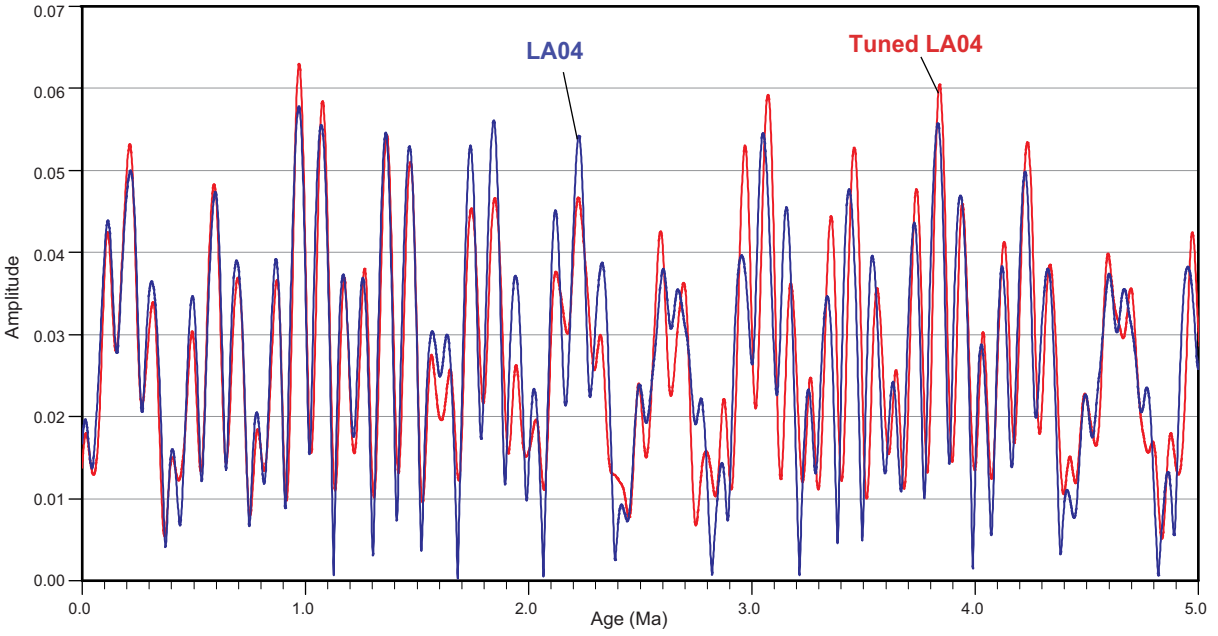

Figure 5: Graph comparing LA04 eccentricity and AROS tuned eccentricity.

A comparison of LA04 eccentricity and AROS tuned eccentricity is provided in Figure 5. The differences are small and there is good age agreement between Orbiton Sequence Boundary 17 and the sequence boundary that occurs one straton below the Permian/Triassic boundary (Al-Husseini and Matthews, 2010a). Untuned, there is no consistent repeat. Indeed, astronomer's uncertainty increases dramatically on the scale of a few tens of millions of years (e.g. Laskar et al., 2004, Figure 20 and Table 8).

ORBITAL-FORCING MODELING OF GLACIO-EUSTATIC SEA-LEVEL FLUCTUATIONS

Parametric Forward Modeling Revisited

A parametric forward model (hereafter, PFM) is intended to be intermediate between simple and complex (Matthews and Frohlich, 2002, p. 515-516). The original paper remains a useful explanation, but the orbital-forcing periods (and thereby sea-level calculations) are based on MFD97 and are also of pre-tuning vintage. Nevertheless, the paper is well-illustrated and will be cited as visual examples.

Figures 6 provides synoptically the crux of the glacio-eustatic PFM *ice cylinder* (model #2.9.1). Table 3 provides a description of glacio-eustatic PFM model parameter space. The math is all piece-wise linear at 1,000 year time steps. The PFM assumes today's continental geometry and a source of low- to mid-latitude reverse thermo-haline ocean circulation somewhere. The parameters of the model can be modified to reflect different geologic times intervals to reflect changing polar continents (e.g. Paleozoic Gondwana at high latitudes).

The most straight-forward parameter in Figure 6b and Table 3 is phase transition point *January insolation at 70° South (critical)*, hereafter (I_S crit). Below this parameter and considering only high-latitude, southern hemisphere effects, each annual cycle would net-accumulate glacial ice, thus lowering global sea level. Above (I_S crit), summer melting in each annual cycle would net-melt glacial ice for each year, thus raising global sea level.

The value of (I_S crit) may be affected by global atmospheric conditions such as greenhouse gases, catastrophic volcanism, meteorite impact, etc., or oceanic effects such as ocean circulation or size of ocean basins (see Immenhauser and Matthews, 2004). These phenomena can all be approximated synoptically by setting *initial sea level* (SL start) higher or lower. But through it all, with any glacial ice

volume on the planet, sea level shall surely be affected by orbital forcing.

Table 3
Sea level modeling parameter space
(See text for discussion)

Ice and Sea level Parameters	
(continent and ice modeled as circular)	
Radius of ice-prone continent	(km)
Max radius of ice sheet	(km)
Height of ice cylinder	(km)
Radius melt belt	(km)
SL max	(-m)
SL min	(-m)
January, 70^{O} South Parameters	
Insolation, South, critical	(Watts/m^2)
MaxIceGrowth rate	(m. ice/yr)
MaxIceMelt rate	(m. ice/yr)
July, 30^{O} North Parameters	
Insolation, North, critical	(Watts/m^2)
MaxIceGrowth rate	(m. ice/yr)
MaxIceMelt rate	(m. ice/yr)
Starting Conditions	
Start Time (1,000 yrs time step)	(Ma)
Start Sea Level	(m. below ice-free)

The next most-straight-forward parameter in Table 3 is *Radius of ice-prone continent* and resultant (SL min, i.e. the maximum lowering of sea level by storing ice on all of the ice-prone continent). This seems simple enough: Antarctica is today squarely beneath the South Pole and ca. 90 m sea-level-equivalent is an outside estimate of all the ice the continent could hold. Results discussed here use only SLmin = -90 m. Clearly, the further back in time, the more uncertain this number becomes. Note well that 70^{O} South neatly encircles Antarctica today, but Northern Hemisphere Pleistocene glaciers extended down to ca. 40^{O} North. Thus, there is room to consider much larger Southern Hemisphere ice sheets back in time.

In Table 3, the height of ice cylinder and melt-belt around glacial ice are set at generalities of modern Antarctica (e.g. Fastook and Prentice, 1994), but can be varied to user's choice.

So, how does July, 30^{O} North figure into this? The *snow gun hypothesis* (Prentice and Matthews, 1991) proposes Northern Hemisphere, mid-latitude reverse thermo-haline ocean circulation on a scale not observed today (Brass et al., 1982; Oglesby, 1989). The model uses July Insolation at 30^{O} North to approximate this effect. Mid- to low-latitude warm, saline sea water sinks to intermediate depths and flows poleward. Warm water upwelling around a cold Antarctic continent begins as a *snow gun* effect (Figure 6a).

In Figure 6b, below (I_N crit), the larger (I_N), the warmer the water upwelling around Antarctica, the more net-annual-accumulation of glacial ice. Above (I_N crit) the still-yet-warmer upwelling water turns the *snow gun* seasonally into a *rain gun*, producing a net-annual-reduction of glacial ice during the model time steps at the higher end of the (I_N) range.

In the calculations of tuned eccentricity and of various sea-level files, dozons (ca. 4.86 My) show similarity, but are not precise repeats. Orbitons (three consecutive dozons; ca. 14.580 My) are nearly precise repeats.

The Straton and the Summing of Sine Waves

The 405 Ky definition of the Straton derives precisely from Term 1 (g2 – g5) in the Fourier representation of eccentricity (Laskar et al., 2004, their table 6; Matthews and Frohlich, 2002, Table 3). When all sine waves are added together over the time of an Orbiton (14.58 My), the average of 36 stratons is precisely 405 Ky. However, the duration of individual stratons varies with a standard deviation on the order of ± 0.05 (e.g. ca. 285 to 505 Ky).

Interestingly, in sea-level modeling, the duration of any particular straton does vary from one sea level parameterization to another. Thus, model/data comparison offers the long-term possibility of finding a global *best fit* sea-level parameterization for each Orbiton or even Dozon throughout geologic time.

Synoptic Results of Grid Search of Parameter Space

An exploratory grid search of the PFM parameter space (I_N crit, I_S crit and SL start) suggests a wide array of sea-level histories to be described in terms of maximum-ice, minimum-ice, flooding intervals (e.g. MFIs). The grid search is reviewed synoptically in AROS terminology (Table 2).

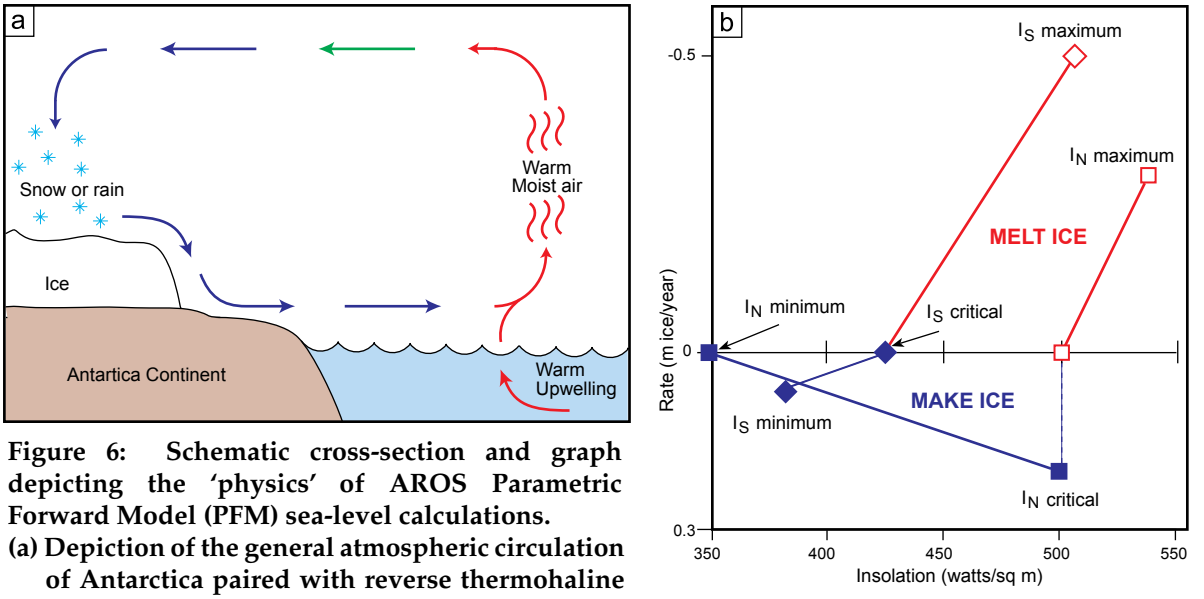

Figure 6: Schematic cross-section and graph depicting the 'physics' of AROS Parametric Forward Model (PFM) sea-level calculations.
(a) Depiction of the general atmospheric circulation of Antarctica paired with reverse thermohaline circulation. Warm water adjacent to a cold continent increases moisture transport to the continent.
(b) The critical role of (I_S critical) and (I_N critical) to the making and melting of the glacier. See text for discussion.

The exploratory grid search produced a wide variety of predictions depending on input parameters. These include: (1) maximum-ice, stable glaciers with change in sea-level of 25–35 m; (2) minimum-ice, stable glaciers with change in sea level of 10–20 m; (3) mid-size, stable glaciers with very pronounced Orbiton low stands and change in sea level of 40–50 m; (4) mid-size, unstable glaciers, which became *stuck* in max-ice mode; and (5) maximum-ice glaciers, which became *un-stuck* and transitioned even to minimum-ice glaciers.

The most persistent features through all of this were regularly-spaced stratons offering 10–15 m higher peak sea levels than adjacent stratons (i.e. MFIs). These are predicted at (proceeding up section) Straton nA-2, nB-2 and nC-2. Lesser flooding events are predicted in Straton nA-8, nA-10, nB-8, nB-10, nC-8, and nC-10. Typical height of these excursions above nearby stratons is 5–10 m.

The grid search suggests sequences boundaries (SB) often occur at the scale of one to three straton-scale lower sea levels followed by an abrupt sea level rise. This is often seen at both Orbiton (14.58 My) and Dozon (4.86 My) scale. The Dozon is prone to a less dramatic division into a lower five-straton short third-order sequence and an upper seven-straton long one.

Special attention was given to effects of parameterization around model-predicted second-order (Orbiton:14.58 My) sequence boundaries. The generality is that, with changing parameters, second-order sequence boundaries develop out of the Dozon (4.86 My) boundaries at SB nA, SB nB and possibly (with evolving boundary conditions) at SB nC (though not yet encountered in the preliminary exploratory grid search).

With sea levels that became unstable, rapid sea-level rises to minimum-ice conditions tended to take off from peak sea levels/MFIs (described above). Likewise, out-of-the-ordinary sea-level falls begin in the bottom of SBs (described above) and keep falling until maximum-ice conditions take over. In either case, the gap between previous sea-level fluctuations and the new, stable mode of sea-level fluctuations is about 30–40 m. In the case of sea-level rise to a new stable mode, this would likely be seen as the sudden appearance of a widespread deeper-water facies above a *MFS*. In the case of sea-level fall to a new stable mode, this dictates an out-of-the-ordinary unconformity, with longer duration depending on local subsidence rates.

FUTURE TRENDS IN STRATIGRAPHY

Stratigraphy continues to make slow but steady progress on the path from *observe and seek to explain* (inductive mode) towards *predict and seek to observe* (deductive mode). Many sequence stratigraphers presently operate in a *modified inductive mode*. They *observe and seek to explain* in the language of *ad hoc* generalities derived from past common experience that predates the current understanding of orbital forcing of glacio-eustasy. These generalities may turn out to be a hindrance to today's geoscientist.

For example, the transgressive systems tract (TST) is traditionally followed by the high-stand systems tract (HST). HST is an *ad hoc* term that unnecessarily implies constant sea level and basinward progradation of laterally-continuous capping facies. Orbital-forcing PFM results suggest the HST to be generally regressive and composed of numerous stratons, each having a unique and significant sea-level amplitude. The term *regressive systems tract* (RST) circumvents the inadvertent and (often?) misleading bias of HST. One's thinking about sequence stratigraphy and exploration plays takes on a whole new dimension.

The term *maximum flooding surface* poses a similar problem. It suggests looking for a more offshore facies to suddenly appear in the section. The PFM generality would be phrased differently. First, yes: an unconformity on any scale will likely be a flooding surface, but *maximum* need not apply. Unconformities at any scale are worthy of note. Elsewhere, numerous *MFSs* in the literature correlate well with PFM peak sea levels that are in the middle of their stratons (Al-Husseini and Matthews, 2010a). To call these MFSs could inadvertently mislead the observer in the field or at well site. These sea-level rises are modeled to be rising at less than one meter per thousand years. In some facies, they may occur as a thickened section, not deeper-water facies. When the term *MFS* pops to mind, think to call it an MFI, or even a *peak sea level* (PSL) and the inadvertent bias is avoided.

The Staton as the tuning fork of geologic time has immediate application to improved dating of unconformities and to how sequence stratigraphers describe what they observe. Biostratigraphers identify faunal discontinuities and take the corresponding surfaces to represent stage boundaries. As discussed in Al-Husseini and Matthews (2010a) these surfaces often do not appear to correspond to sequence boundaries. What the explorationist would really like to know is the precise straton number of sediments above and below the sequence boundary and correlative conformity. This will require that the biostratigraphers place their dates in the context of stratons, MFIs, etc. that can be correlated worldwide.

Fifty years ago, stratigraphers *observed* transgressions and knew only that the explanation lay in basin subsidence or sea-level rise. But having said that, stratigraphers didn't know where to go. Along came plate tectonics (Vine and [D.H.] Matthews, 1963). Ten years later, plate tectonics began to explain many stratigraphic observations (e.g. Watts and Ryan, 1976). Now most stratigraphers naturally think, at least qualitatively, in a plate tectonics context.

Today, our knowledge regards orbital forcing of Earth's ocean-atmosphere-cryosphere system is about where plate tectonics was 40 years ago. By analogy, the next 10 years should see improvements in the ways stratigraphy is observed and explained.

ACKNOWLEDGEMENTS

We thank Cliff Frohlich and Bill Hutson participation in the RKM & Associates tune-up process. The authors thank Nestor A. Buhay II for designing the graphics for this manuscript.

REFERENCES

Al-Husseini, M.I. 2008. Launch of the Middle East Geologic Time Scale. GeoArabia, v. 13, no. 4, p. 11 and 185-188.

Al-Husseini, M.I. and R.K Matthews 2005. Arabian Orbital Stratigraphy: Periodic second-order sequence boundaries. GeoArabia, v. 10, no. 2, p 165-184.

Al-Husseini, M.I. and R.K. Matthews 2006. Devonian Jauf Formation, Saudi Arabia: Orbital Second-order Depositional Sequence 28. GeoArabia, v. 11, no. 2, p. 53-70.

Al-Husseini, M.I. and R.K. Matthews 2008. Jurassic-Cretaceous Arabian orbital stratigraphy: The AROS-JK Chart. GeoArabia, v. 13, no. 1, p. 89-94.
Al-Husseini, M.I. and R.K. Matthews 2010a. Calibrating Mid-Permian to Early Triassic Khuff Sequences with orbital clocks. GeoArabia, v. 15, no. 3, p. 171-206.
Al-Husseini, M.I. and R.K. Matthews 2010b. Tuning Late Barremian – Aptian Arabian Plate and global sequences with orbital periods. In F.S.P. van Buchem, M.I. Al-Husseini, F. Maurer and H.J. Droste (Eds.), Barremian - Aptian stratigraphy and hydrocarbon habitat of the eastern Arabian Plate. GeoArabia Special Publication 4, Gulf PetroLink, Bahrain, v. 1, p. 199-228.
Berger, A.L. and M.F. Loutre 1991. Insolation values for the climate of the last 10 million years. Quaternary Science Reviews, v. 10, p. 297-317.
Brass, G.W., J.R. Southam and W.H. Peterson 1982. Warm Saline Bottom Water. Nature, v. 296, p. 620-623.
Fastook, J.L. and M. Prentice 1994. A finite-element model of Antarctica: sensitivity test for meteorological mass-balance relationship. Journal of Glaciology, v. 40, p. 167-175.
Immenhauser, A. and R.K. Matthews 2004. Albian sea-level cycles in Oman: The 'Rosetta Stone' approach. GeoArabia, v. 9, no. 3, p. 11-46.
Laskar, J. 1990. The chaotic motion of the Solar System: a numerical estimate of the size of the chaotic zones. Icarus, v. 88, p. 266-291.
Laskar, J. 1999. The limits of Earth orbital calculations for geological time-scale use. Philosophical Transactions of the Royal Society of London, v. 357, p. 1735-1760.
Laskar, J., P. Robutel, F. Joutel, M. Gstineau, A.C.M. Correia, and B. Levrard 2004. A long-term numerical solution for the insolation quantities of the Earth. Astronomy and Astrophysics, v. 428, p. 261-285.
Matthews, R.K., C. Frohlich and A. Duffy 1997. Orbital forcing of global change throughout the Phanerozoic: A possible stratigraphic solution to the eccentricity phase problem. Geology, v. 25, p. 807-810.
Matthews, R.K. and C.F. Frohlich 2002. Maximum flooding surface and sequence boundaries: comparisons between observation and orbital forcing in the Cretaceous and Jurassic (65-190 Ma). GeoArabia, v. 7, no. 3, p. 503-538.
Prentice, M.L. and R.K. Matthews 1991. Tertiary ice sheet dynamics: The snow gun hypothesis. Journal of Geophysical Research, v. 96, no. B4, p. 6811-6827.
Oglesby, R.J. 1989. A GCM study of Antarctic glaciation. Climate Dynamics, v. 3, p. 135-156.
Watts, A.B. and W.B.F. Ryan 1976. Flexure of the lithosphere and continental margin basins. Tectonophysics, v. 36, p. 25-44.
Vine, F. J. and D.H. Matthews 1963. Magnetic anomalies over oceanic ridges. Nature, v. 199 (4897), p. 947-949.

ABOUT THE AUTHORS

Robley K. Matthews *is Professor of Geological Sciences at Brown University, Rhode Island, USA, and is general partner of RKM & Associates. Since the start of his career in the mid 1960s, he has had experience in carbonate sedimentation and diagenesis and their application to petroleum exploration and reservoir charcterization. Rob's current interests center around the use of computer-based dynamic models in stratigraphic simulation.*

rkm@brown.edu

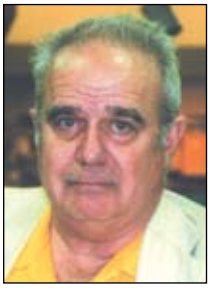

Moujahed I. Al-Husseini *founded Gulf PetroLink in 1993 in Manama, Bahrain. Gulf PetroLink is a consultancy aimed at transferring technology to the Middle East petroleum industry. Moujahed received his BSc in Engineering Science from King Fahd University of Petroleum and Minerals in Dhahran (1971), MSc in Operations Research from Stanford University, California (1972), PhD in Earth Sciences from Brown University, Rhode Island (1975) and Program for Management Development from Harvard University, Boston (1987). Moujahed joined Saudi Aramco in 1976 and was the Exploration Manager from 1989 to 1992. In 1996, Gulf PetroLink launched the journal of Middle East Petroleum Geosciences, GeoArabia, for which Moujahed is Editor-in-Chief. Moujahed also represented the GEO Conference Secretariat, Gulf PetroLink-GeoArabia in Bahrain from 1999-2004. He has published about 50 papers covering seismology, exploration and the regional geology of the Middle East, and is a member of the EAGE and the Geological Society of London.*

geoarabi@batelco.com.bh